THE JOURNAL OF PHYSICAL CHEMISTRY LETTERS
A JOURNAL OF THE AMERICAN CHEMICAL SOCIETY

Open Access
This article is licensed under CC-BY-NC-ND 4.0

pubs.acs.org/JPCL
Letter

How Crystal Size and Number Steer Asymmetric Crystallization

Sjoerd W. van Dongen,[‖] Pepijn J. Rang,[‖] Karin G.P. Dautzenberg, Bernard Kaptein, and Willem L. Noorduin*

Cite This: https://doi.org/10.1021/acs.jpclett.5c03059
Read Online

ACCESS | Metrics & More | Article Recommendations | Supporting Information

ABSTRACT: Chiral amplification processes during crystallization can hinge on subtle asymmetries in crystal populations, yet the underlying kinetic drivers remain elusive. Here we experimentally investigate how size and mass imbalances between two enantiomeric crystal populations translate to asymmetric growth rates that determine asymmetric crystal growth. We find that the interplay between imbalances in size and mass can yield positive, linear or even negative nonlinear chiral amplification. Consequently, though small crystals have a thermodynamically higher solubility than large ones, a minority population of small crystals can collectively outgrow and ultimately dominate a majority of larger crystals. This amplification due to size effects can be further enhanced or dampened by controlling growth rates. Our findings uncover an intricate kinetic selection mechanism driven by population-level growth rates and governed by fundamental crystallization dynamics. Together, these results provide new insights into the origin of nonlinear amplification phenomena and offer practical guidance for competitive asymmetric crystallization and self-assembly processes.

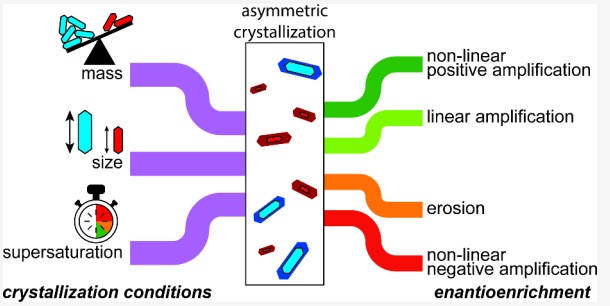

Downloaded via AMOLF on January 19, 2026 at 12:29:08 (UTC).
See https://pubs.acs.org/sharingguidelines for options on how to legitimately share published articles.

Asymmetric crystallization processes are of profound importance for both fundamental science and practical applications with wide use in the pharmaceutical and fine chemical industries.[1−8] Especially interesting is the asymmetric crystallization of chiral molecules into enantiomerically pure crystals (so-called conglomerates).[9−20] Under racemizing conditions, the enantiomers can interconvert in the liquid phase and thereby form a common resource pool for asymmetric crystallization. An initial enantioenrichment in the solid phase can then be amplified through cycles of crystal growth and dissolution, allowing full deracemization. While the key prerequisites for such deracemizations are well-established, recent studies have revealed complex nonlinear effects that can occur during asymmetric crystallization, which profoundly influence the selectivity and efficiency of chiral amplification.[21−25]

In particular, differences in the growth rates of enantiomeric crystal populations can spontaneously enrich one enantiomer over the other. It remains unclear, however, where such growth-rate asymmetries originate and how they can be leveraged and controlled. Several studies have shown that larger crystals generally grow faster and are thermodynamically more stable than their smaller counterparts, which has been proposed as a method to break symmetry and drive chiral amplification.[26−31] Moreover, it is known that crystal morphology and the evolution thereof can influence crystal growth rates.[32,33] Although the kinetics of individual crystal growth have been studied in detail,[34] our understanding of how large, heterogeneous populations of interacting crystals behave collectively during crystallization is still limited. Such insights are of key importance for chiral crystallizations, as even minor differences in crystal size or morphology between enantiomeric populations can lead to significant divergence in their growth dynamics and, consequently, in the resulting chiral purity of the solid phase.

This raises an important question: how does the competition between two enantiomeric crystal populations for a common racemizing solute pool translate into asymmetric crystallization outcomes? More specifically, how do differences in initial mass and crystal size—two interrelated yet independently tunable parameters—govern the net growth rates of the enantiomer populations and determine the direction and extent of chiral amplification within a single growth step?

This question is particularly relevant because crystal size disparities frequently arise spontaneously through nucleation, Ostwald ripening, or growth-rate dispersion.[35,36] Such size disparities can also be introduced actively through seeding, mechanical grinding, or controlled crystallization conditions. Hence, understanding the consequences of size disparities on the growth rates of crystal population is essential not only to

Received: September 30, 2025
Revised: January 3, 2026
Accepted: January 5, 2026

ACS Publications
© XXXX The Authors. Published by American Chemical Society

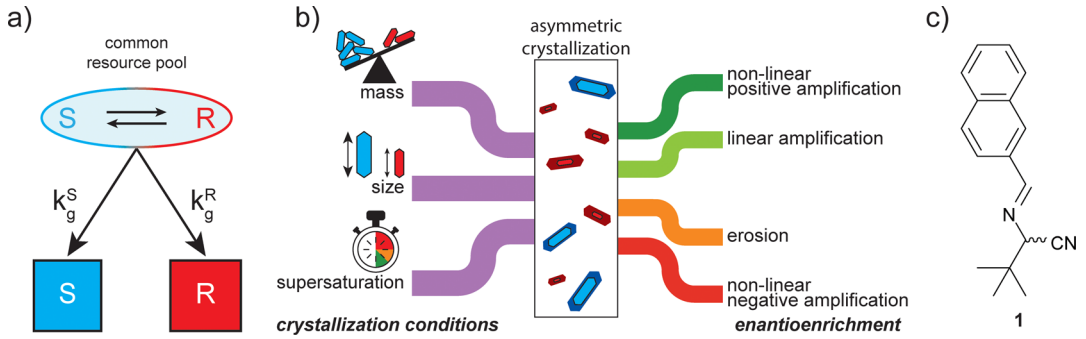

Figure 1. Asymmetric crystallization is dominated by the fastest growing population. (a) Conglomerates crystallize as two populations of enantiopure crystals with growth rates k_g^R and k_g^S, respectively. Racemization in solution creates a common resource pool. (b) The outcome of asymmetric crystallization is determined by the balance of the collective growth rate of the crystal populations through the number of crystals (via mass), their size, and the crystallization conditions (supersaturation). (c) Racemizable conglomerate **1**.

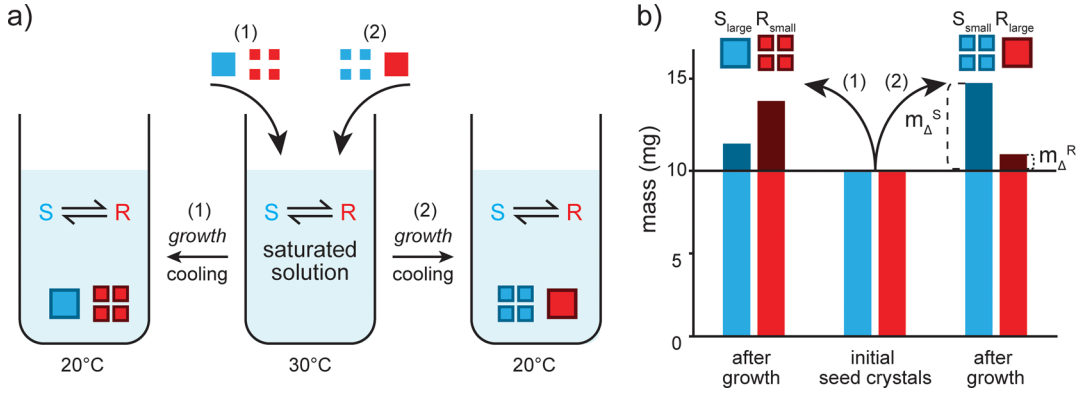

Figure 2. Chiral crystallization for equal masses but different crystal sizes of each enantiomer population. (a) Seeded growth of enantiomer populations under racemizing conditions from a saturated solution through cooling. (b) Crystal populations of equal mass but unequal size exhibit asymmetric growth rates, favoring the enantiomer population composed of smaller crystals.

elucidate the fundamental principles of chiral crystallization but also to develop rational strategies that steer deracemization toward the desired outcome.

In this work, we experimentally investigate how differences in crystal size and population mass affect the outcome of asymmetric crystal growth under racemizing conditions. By carefully preparing enantiomeric seed mixtures that differ in either size or mass—or both—we can modulate the solid phase enantioenrichment and growth rate of each population independently. Moreover, motivated by fundamental insights on the mechanisms of crystal growth, we show that the effects of crystal size disparities can be further manipulated through the applied supersaturation. Collectively, our findings highlight the domination of the fastest growing population, a core principle that prompts us to rethink how to understand, design, and control asymmetric crystallization processes.

To investigate how size differences between two otherwise identical crystal populations influence the population growth rates and the outcome of asymmetric crystallization, we prepared both small and large seed crystals of both the (*R*) and (*S*)-enantiomer of **1** (Figure 1c), a well-established racemizable conglomerate.[37] Small seed crystals (10−20 μm) were obtained by mechanical grinding assisted by ultrasonication in the presence of glass beads.[38] Large seed crystals (30−50 μm) were obtained by growing the small crystals (detailed procedures and characterization data for both small and large seed crystal batches are provided in the Supporting Information).

For our first experiment, using these small and large seed crystals, two types of racemic mixtures (i.e., no net solid-phase enantioenrichment) were prepared such that each enantiomer had equal mass, but a different crystal size compared to its counterpart. We combined (1) large (*S*)-enantiomer crystals with small (*R*)-enantiomer crystals, and (2) large *R* crystals mixed with small *S* crystals. These crystal mixtures were subsequently added as seed crystals to a saturated, racemizing solution of **1** in methanol at 30 °C, containing 50 μL/mL basic racemization catalyst 1,8-diazabicyclo[5.4.0]undec-7-ene (DBU) (Figure 2a). Crystal growth was initiated by slowly cooling the solution with 0.22 °C/min to 20 °C. To keep attrition effects to a minimum during growth, the solution was shaken instead of stirred.

To determine how much of each enantiomer population crystallized, the resulting solids were isolated through vacuum filtration and their composition was determined using chiral HPLC. Importantly, the entire cooling trajectory was performed within the metastable zone, such that nucleation is minimized and precipitation from the supersaturated solution is dominated by growth of the seed crystals.

Before growth, both the population of small and large crystals have equal mass. After growth, as expected, both populations have gained mass, but not in equal amounts: the population with the smaller seed crystals grew more than the one with large seed crystals (Figure 2b). Hence, the population of small crystals must have grown faster than the population of larger crystals. This size dependency of enantioenrichment is

https://doi.org/10.1021/acs.jpclett.5c03059
J. Phys. Chem. Lett. XXXX, XXX, XXX−XXX

nontrivial. The Gibbs−Thomson effect thermodynamically favors the growth of large crystals, such that the small crystals are individually less stable. However, under kinetic, out-of-equilibrium conditions the small crystal population can feature a higher collective growth rate because of a larger combined surface area.[26,35]

For populations of equal mass, we thus find that a disparity in crystal size between two enantiomer populations breaks symmetry in favor of the smaller crystals. Commonly, however, chiral amplification is directed by breaking symmetry through unequal initial solid masses, such that the population with larger mass (the major enantiomer) wins at the cost of the population with smaller mass (the minor enantiomer). When chiral amplification is directed through mass imbalances, the sizes of crystal populations are oftentimes neglected or simply assumed to be the same. As we have just demonstrated, however, crystal sizes are important. Moreover, the imbalance of populations in mass can differ from the imbalance in size. We foresee the complex interplay of imbalances in mass and size can thus enhance but also diminish chiral amplification of the desired enantiomer.

To analyze how an interplay between size and mass affects chiral amplification, we determine the mass that is grown onto each population (m_Δ^R and m_Δ^S)), calculate the enantiomeric excess of the crystallized material ($ee_\Delta = (m_\Delta^R - m_\Delta^S)/(m_\Delta^R + m_\Delta^S)$), and define the amplification factor (α) as ee_Δ relative to the initial mass imbalance (ee_0):

$$\alpha = \frac{ee_\Delta}{ee_0}$$

Akin to Kagan's analysis of asymmetric catalysis,[39] this amplification factor classifies asymmetric crystallization into four distinct regimes. When $\alpha = 1$, both populations grow in proportion to their initial mass imbalance: the *ee* of grown material is equal to the starting *ee*, resulting in linear amplification. When $\alpha > 1$, the major population in mass grows faster than the minority population, resulting in nonlinear amplification of the major enantiomer. When $0 < \alpha < 1$, the major enantiomer grows faster than the minority, but insufficiently as to maintain its starting enantioenrichment, thus resulting in net erosion of the initial *ee*. When $\alpha < 0$, the minority enantiomer grows faster than the majority enantiomer, resulting in negative nonlinear amplification.

Using a constant imbalance in seed mass (ee_0 = 20% in *R*), we prepared five experimental imbalances in size by mixing small and large crystals of the two enantiomers (see the Supporting Information for details): (i) all majority enantiomer crystals are larger than the minority enantiomer crystals (i.e., majority larger), (ii) only the majority crystals that make up the enantiomeric excess are larger (i.e., excess larger), (iii) all crystals are of equal size, (iv) the excess crystals are smaller, and (v) all majority crystals are smaller than the minority enantiomer crystals (Figure 3a). Subsequently, each mixture was used to seed a racemizing clear supersaturated solution to induce growth (see the Supporting Information for details).

The crystallized solid was analyzed as before and α was determined (Figure 3b). For crystals of equal sizes, we observe near-linear amplification ($\alpha \approx 1$). Although nucleation and small inherent size disparities between seed crystals slightly suppress amplification (see the Supporting Information for details), the populations grew with rates that are approximately proportional to their initial mass—as expected in the absence

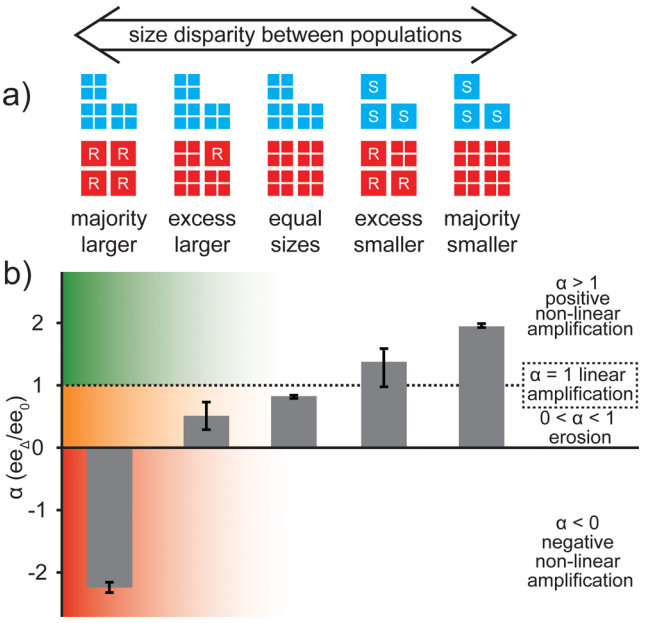

Figure 3. Asymmetric crystallization directed by crystal size disparity. (a) Initial seeds are enriched in (*R*)-**1** by mass, but both enantiomer populations have different crystal sizes. (b) Maintaining the initial enantioenrichment in mass through growth constitutes expected linear amplification. However, crystal-size disparity in asymmetric crystallization can cause positive nonlinear chiral amplification, linear amplification, erosion, or even negative nonlinear amplification, characterized by amplification factor α.

of any size imbalance. When all majority crystals are smaller than the minority crystals, we observe strong positive nonlinear amplification ($\alpha \gg 1$): the majority population grows much faster due to the smaller size of its constituting crystals.

Conversely, when the majority crystals are larger than the minority, we observe strong negative nonlinear amplification ($\alpha \ll 0$): the minor enantiomer—through its larger collective surface area—has now completely outgrown the majority enantiomer. Despite the same significant initial *ee* in *R* by mass, switching the size imbalance from majority smaller to majority larger crystals thus fully reverses the outcome of chiral amplification: from amplifying the major ($\alpha \approx +2$, final *ee* = 80% in *R*) to amplifying the minor enantiomer ($\alpha \approx -2$, final *ee* = 3% in *R*). Hence, through the domination of the fast-growing population, the size imbalance completely determines the outcome of asymmetric crystallization.

Consistent with these findings, selectively changing only the size of the crystals constituting the excess (i.e., excess smaller vs excess larger), yields similar relative effects of the size imbalance on chiral amplification, although less pronounced (Figure 3). Smaller excess crystals still give positive nonlinear amplification ($\alpha \approx 1.5$), but larger excess crystals now yield erosion ($\alpha \approx 0.5$), a much weaker effect than the negative nonlinear amplification previously observed when all majority crystals were larger. These weaker effects on amplification observed when changing only the relative size of the excess crystals—rather than the whole population—can be explained by the smaller imbalances in the total surface area between the populations. These results demonstrate that strategic preparation of the initial solid phase—specifically, incorporating many small enantiopure seed crystals with large cumulative surface area—can achieve higher chiral amplification efficiency and thereby accelerate deracemization kinetics.

https://doi.org/10.1021/acs.jpclett.5c03059
J. Phys. Chem. Lett. XXXX, XXX, XXX−XXX

Fundamentally, the outcome of asymmetric crystallization is governed by differences in the growth rates of competing enantiomeric crystal populations. These growth rates are not only influenced by differences in size (r) and mass, but also by the growth mechanism, which in turn depends strongly on the supersaturation of the solution. At low supersaturation, often associated with spiral growth mechanisms, molecular attachment occurs predominantly at energetically favorable sites such as screw dislocations. In this regime, the number of active growth sites—proportional to the number of crystals (N)—determines the population growth rate ($k_g \sim N \sim 1/r^3$).[40] At high supersaturation, often associated with polynuclear and rough growth mechanisms, molecular attachment occurs across the entire surface. In this surface-integration-limited regime, the incorporation of molecules on the crystal surface (A) is rate-limiting ($k_g \sim \Sigma A \sim 1/r$). Indeed, calculations suggest that high supersaturation dampens the effects of size imbalances on population growth rates (Figure 4a, details in the Supporting Information).[41] Furthermore, these calculations show that a small initial size disparity ratio between seed crystal populations has disproportionately large effects on the outcome of asymmetric crystallization (Figure S-9).

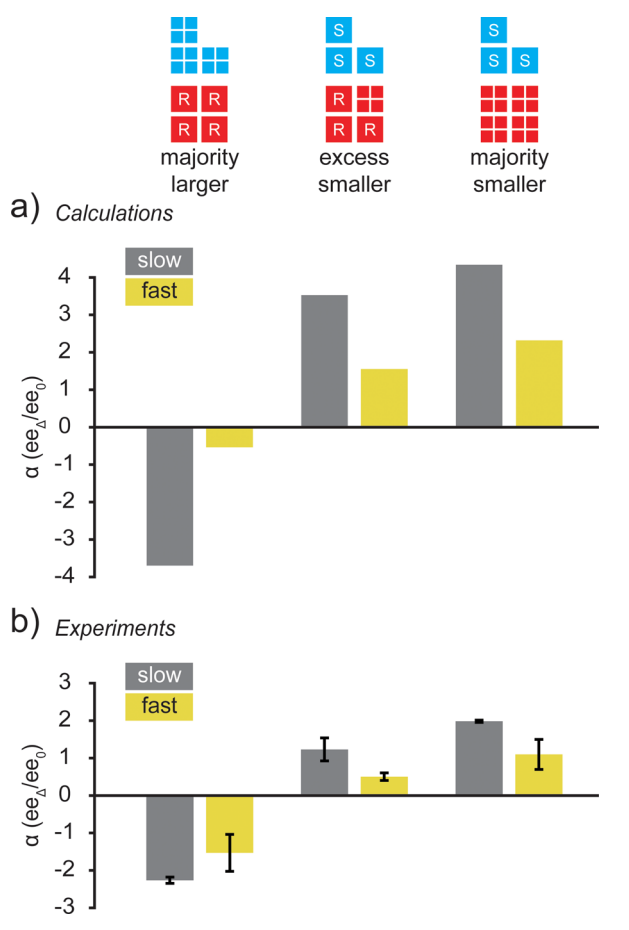

Figure 4. Asymmetric amplification as function of the crystallization rate (through supersaturation). (a) Calculations suggest that, for low supersaturation (slow growth, gray), population growth rate is proportional to the number of crystals. For high supersaturation (fast growth, yellow), population growth rate is surface-integration-limited. (b) Experiments confirm the effect of supersaturation and show that size-induced amplification effects are dampened through fast growth at high supersaturation.

To test how these distinct growth regimes influence the effects of crystal size disparity, we performed asymmetric crystallization experiments under both low supersaturation (achieved by slow cooling from 30 to 20 °C at 0.22 °C/min) and high supersaturation (achieved by fast cooling over the same temperature range at 2 °C/min). As shown in Figure 4b, under slow cooling strong size-dependent chiral amplification is observed, with populations of small crystals growing significantly faster and dominating the solid phase composition. However, under fast cooling, this amplification effect is markedly dampened. This confirms that size disparity effects are more pronounced under surface-integration-limited growth at low supersaturation compared to high supersaturation.

In summary, this study experimentally reveals how subtle disparities in crystal size can decisively impact the outcome of asymmetric crystal growth when populations compete for the same resources. Populations of smaller crystals exhibit higher collective growth rates due to their greater cumulative surface area, enabling them to outcompete larger, thermodynamically more stable crystals. Consequently, disparities in crystal size and mass can enhance, diminish, or even reverse initial enantiomeric imbalances, resulting in regimes of positive, linear, and negative nonlinear amplification.

In this study we have treated crystals as unidimensional and have not aimed to give a full quantitative description. Indeed, facet-dependent growth mechanisms and crystals undergoing morphological changes over time also likely influence the degree of amplification, especially across different supersaturation regimes.[33,42,43] Future studies integrating *in situ* imaging for the tracking of shape and size of individual populations and population-balance modeling should therefore further clarify how size, shape, and growth mechanism interact to control chiral selection.[44,45]

Although we here only study chiral amplification during crystal growth, these results may also help to rationalize empirical trends in deracemization by growth/dissolution cycles such as temperature cycling-induced deracemization.[46] With each cycle, ripening phenomena shift the population size distributions, potentially giving rise to antagonistic size disparities that slow the exponential deracemization kinetics. Different routes exist to counteract this deceleration of deracemization. One known route to maintain the deracemization rate is progressively dampening the temperature swing with every cycle.[46] Our findings rationalize this strategy, which gradually transitions from classic temperature cycles, for which the emerging size disparity increasingly disfavors the major enantiomer, to an accelerated Ostwald-ripening regime, where thermodynamics dominates and the remaining few minor enantiomer crystals are effectively converted. Counterintuitively, we propose exponential deracemization kinetics may also be maintained by progressively increasing crystallization rates during later cycles, as faster crystallization dampens antagonistic size-disparity effects.

Our results also serve as a practical guide for seeding and crystal size control. When a deracemization starts with racemization during growth, using an enantiopure excess comprised of small seed crystals is beneficial. The reverse is true for dissolution: small crystals dissolve faster than a population of large crystals and will thus experience negative amplification. A cyclic process starting with racemization during dissolution would thus benefit from an enantiopure excess comprised of large crystals and racemic bulk material comprised of small seed crystals. This lesson is also grounded

https://doi.org/10.1021/acs.jpclett.5c03059
J. Phys. Chem. Lett. XXXX, XXX, XXX−XXX

in theory: if $ee_0 = 0$, the population with the greatest size deviation is enriched.[47] Similar is true for attrition-based deracemizations (Viedma ripening): if $ee_0 = 0$, the population with the larger crystals determines the outcome of deracemization.[48] Our results further imply that intermittent grinding could be effective to mitigate undesired ripening by resetting the crystal size distribution, which is even more powerful when combined with monitoring the crystal size distribution.[49,50] Finally, the use of small crystals may mitigate undesired growth inhibition from impurities.[51,52]

Overall, this work underscores that crystal size is a critical yet often overlooked kinetic parameter in asymmetric crystal growth. Size disparities can be deliberate or accidental: many small crystals can for instance arise through nucleation and have a disproportionally big impact because of their high collective growth rate.[53] We also note that any process mixing two or more sources of crystals (e.g., a racemic mixture of crystals and enantiopure crystals to establish an enantiomeric excess) invariably encounters size disparities. Unfortunately, literature often lacks details on the preparation and origin of seed crystals used in crystallization experiments. Because subtle disparities quickly arise and can have major effects, this omission in reporting prevents comparing between studies and hampers benchmarking crystallization processes. At best, deracemization is faster and completely reproducible. At worst, neglecting seed design may lead to confusing, inexplicable or irreproducible results. Furthermore, special care should be taken when re-using material from a completed batch in a subsequent crystallization, as dramatic changes in crystal properties (e.g., size, morphology) may occur. Hence, deliberate and well-reported seed design is essential for reproducibility and mechanistic understanding.

Finally, these findings on thermodynamically equal populations prompt a broader question: how does the kinetic domination of the fastest-growing population influence crystallization when the competing phases differ in thermodynamic stability?[54,55] This principle could be harnessed to deracemize the many chiral molecules that crystallize not as conglomerates but as racemic compounds.[56−58] In such systems, the enantiopure phase is typically less stable. However, enantiopure crystals might intrinsically grow faster than their racemic counterparts—a parameter so far seldomly considered—or could be actively favored through the choice of seed crystals, analogous to the experiments here. To what extent cleverly exploiting crystal growth kinetics can overcome fundamental thermodynamic limitations is a compelling question. Beyond crystallization, these concepts may extend to the assembly of biological complexes and dynamic supramolecular systems.[59−63]

■ ASSOCIATED CONTENT

Supporting Information

The Supporting Information is available free of charge at https://pubs.acs.org/doi/10.1021/acs.jpclett.5c03059.

General remarks, HPLC analysis, calibration curve, seed crystal preparation, size comparison, SEM and optical microscopy images, size distribution, growth experiments, chromatograms, temperature dependent solubility curves, comparison of crystal growth, and calculation details (PDF)

■ AUTHOR INFORMATION

Corresponding Author

Willem L. Noorduin − *AMOLF, 1098 XG Amsterdam, The Netherlands; Van 't Hoff Institute for Molecular Sciences, University of Amsterdam, 1098 XH Amsterdam, The Netherlands;* orcid.org/0000-0003-0028-2354; Email: noorduin@amolf.nl

Authors

Sjoerd W. van Dongen − *AMOLF, 1098 XG Amsterdam, The Netherlands;* orcid.org/0000-0003-3617-5614

Pepijn J. Rang − *AMOLF, 1098 XG Amsterdam, The Netherlands*

Karin G.P. Dautzenberg − *InnoSyn, 6167 RD Geleen, The Netherlands*

Bernard Kaptein − *InnoSyn, 6167 RD Geleen, The Netherlands*

Complete contact information is available at: https://pubs.acs.org/10.1021/acs.jpclett.5c03059

Author Contributions

‖S.W.v.D. and P.J.R. contributed equally. The manuscript was written through contributions of all authors. All authors have given approval to the final version of the manuscript.

Notes

The authors declare no competing financial interest.

■ ACKNOWLEDGMENTS

P.J.R. and W.L.N. acknowledge funding from the European Research Council (Consolidator Grant No. 101044764-CHIRAL). S.W.vD. acknowledges funding from OCENW.-KLEIN.155, which is financed by the Dutch Research Council (NWO).

■ REFERENCES

(1) Gellman, A. J.; Ernst, K. H. Chiral autocatalysis and mirror symmetry breaking. *Catal. Lett.* **2018**, *148*, 1610−1621.

(2) Frank, F. C. On spontaneous asymmetric synthesis. *Biochim. Biophys. Acta* **1953**, *11*, 459−463.

(3) Srisanga, S.; Flood, A. E.; Galbraith, S. C.; Rugmai, S.; Soontaranon, S.; Ulrich, J. Crystal growth rate dispersion versus size-dependent crystal growth: appropriate modeling for crystallization processes. *Cryst. Growth Des.* **2015**, *15*, 2330−2336.

(4) Klussmann, M.; Iwamura, H.; Mathew, S. P.; Wells, D. H.; Pandya, U.; Armstrong, A.; Blackmond, D. G. Thermodynamic control of asymmetric amplification in amino acid catalysis. *Nature* **2006**, *441*, 621−623.

(5) Sacchi, P.; Wright, S. E.; Neoptolemou, P.; Lampronti, G. I.; Rajagopalan, A. K.; Kras, W.; Evans, C. L.; Hodgkinson, P.; Cruz-Cabeza, A. J. Crystal size, shape, and conformational changes drive both the disappearance and reappearance of ritonavir. *Proc. Natl. Acad. Sci. U. S. A.* **2024**, *121*, No. e2319127121.

(6) Brands, K. M. J.; Davies, A. J. Crystallization-induced diastereomer transformations. *Chem. Rev.* **2006**, *106*, 2711−2733.

(7) Viedma, C.; Cuccia, L. A.; McTaggart, A.; Kahr, B.; Martin, A. T.; McBride, J. M.; Cintas, P. Oriented attachment by enantioselective facet recognition in millimeter-sized gypsum crystals. *Chem. Commun.* **2016**, *52*, 11673−11676.

(8) Murakami, H. From racemates to single enantiomers - chiral synthetic drugs over the last 20 years. *Top. Curr. Chem.* **2006**, *269*, 273−299.

(9) Choi, H. S.; Oh, I. H.; Zhang, B.; Coquerel, G.; Kim, W.; Park, B. J. Chiral flipping in Viedma deracemization. *J. Phys. Chem. Lett.* **2024**, *15*, 4367−4374.

(10) Ma, A.; Du, W.; Wang, J.; Jiang, K.; Zhang, C.; Sheng, W.; Zhang, H.; Jin, R.; Wang, S. Transforming silver nanoclusters from racemic to homochiral via seeded crystallization. *J. Phys. Chem. Lett.* **2023**, *14*, 5095−5101.
(11) Bak, S. Y.; Coquerel, G.; Kim, W.; Park, B. J. Solution volume effects on spontaneous chiral symmetry breaking of sodium chlorate crystals. *J. Phys. Chem. Lett.* **2023**, *14*, 785−790.
(12) Fasel, R.; Parschau, M.; Ernst, K. H. Amplification of chirality in two-dimensional enantiomorphous lattices. *Nature* **2006**, *439*, 449−452.
(13) Hein, J. E.; Huynh Cao, B.; Viedma, C.; Kellogg, R. M.; Blackmond, D. G. Pasteur's Tweezers revisited: On the mechanism of attrition-enhanced deracemization and resolution of chiral conglomerate. *J. Am. Chem. Soc.* **2012**, *134*, 12629−12636.
(14) Ahn, J.; Kim, D. H.; Coquerel, G.; Kim, W. S. Chiral symmetry breaking and deracemization of sodium chlorate in Turbulent Flow. *Cryst. Growth Des.* **2018**, *18*, 297−306.
(15) Srisanga, S.; ter Horst, J. H. Racemic compound, conglomerate, or solid solution: phase diagram screening of chiral compounds. *Cryst. Growth Des.* **2010**, *10*, 1808−1812.
(16) Sakamoto, M.; Fujita, K.; Yagishita, F.; Unosawa, A.; Mino, T.; Tsutomu, T. Kinetic resolution of racemic amines using provisional molecular chirality generated by spontaneous crystallization. *Chem. Commun.* **2011**, *47*, 4267−4269.
(17) Ribó, J. M.; Hochberg, D.; Buhse, T.; Micheau, J. C. Viedma deracemization mechanisms in self-assembly processes. *Phys. Chem. Chem. Phys.* **2025**, *27*, 2516−2527.
(18) Kondepudi, D. K.; Kaufman, R. J.; Singh, N. Chiral symmetry breaking in sodium chlorate crystallization. *Science* **1990**, *250*, 975−976.
(19) Palmans, A. R. A. Deracemisations under kinetic and thermodynamic control. *Mol. Syst. Des. Eng.* **2017**, *2*, 34−46.
(20) Breveglieri, F.; Maggioni, G. M.; Mazzotti, M. Deracemization of NMPA via temperature cycles. *Cryst. Growth Des.* **2018**, *18*, 1873−1881.
(21) Zhang, B.; Coquerel, G.; Kim, W. S. Isothermal deracemization of sodium chlorate in an agitated reactor: the effect of crystal size variables. *Cryst. Growth Des.* **2023**, *23*, 741−750.
(22) Deck, L. T.; Hosseinalipour, M. S.; Mazzotti, M. Exact and ubiquitous condition for solid-state deracemization in Vitro and in Nature. *J. Am. Chem. Soc.* **2024**, *146*, 3872−3882.
(23) Buhse, T.; Cruz, J. M.; Noble-Terán, M. E.; Hochberg, D.; Ribó, J. M.; Crusats, J.; Micheau, J. C. Spontaneous deracemizations. *Chem. Rev.* **2021**, *121*, 2147−2229.
(24) van Dongen, S. W.; Ahlal, I.; Leeman, M.; Kaptein, B.; Kellogg, R. M.; Baglai, I.; Noorduin, W. L. Chiral amplification through the interplay of racemizing conditions and asymmetric crystal growth. *J. Am. Chem. Soc.* **2023**, *145*, 436−442.
(25) Uwaha, M. A model for complete chiral crystallization. *J. Phys. Soc. Jpn.* **2004**, *73*, 2601−2603.
(26) Chernov, A. A. *Modern Crystallography III*, 1st ed.; Springer: Berlin, Heidelberg, 1984.
(27) Kile, D. E.; Eberl, D. D.; Hoch, A. R.; Reddy, M. M. An assessment of calcite crystal growth mechanisms based on crystal size distributions. *Geochim. Cosmochim. Acta* **2000**, *64*, 2937−2950.
(28) van Rosmalen, G. M.; Daudey, P. J.; Marchee, W. G. J. An analysis of growth experiments of gypsum salts in suspension. *J. Cryst. Growth* **1981**, *52*, 801−811.
(29) de Goede, R.; van Rosmalen, G. M. Modelling of crystal growth kinetics: a simple but illustrative approach. *J. Cryst. Growth* **1990**, *104*, 392−398.
(30) Eek, R. A.; Dijkstra, S.; van Rosmalen, G. M. Dynamic modeling of suspension crystallizers, using experimental data. *AIChE J.* **1995**, *41*, 571−584.
(31) Noorduin, W. L.; Vlieg, E.; Kellogg, R. M.; Kaptein, B. From Ostwald ripening to single chirality. *Angew. Chem., Int. Ed.* **2009**, *48*, 9600−9606.
(32) Neugebauer, P.; Cardona, J.; Besenhard, M. O.; Peter, A.; Gruber-Woelfler, H.; Tachtatzis, C.; Cleary, A.; Andonovic, I.; Sefcik, J.; Khinast, J. G. Crystal shape modification via cycles of growth and dissolution in a tubular crystallizer. *Cryst. Growth Des.* **2018**, *18*, 4403−4415.
(33) Snyder, R. C.; Doherty, M. F. Faceted crystal shape evolution during dissolution or growth. *AIChE J.* **2007**, *53*, 1337−1348.
(34) di Gregorio, M. C.; Elsousou, M.; Wen, Q.; Shimon, L. J. W.; Brumfeld, V.; Houben, L.; Lahav, M.; van der Boom, M. E. Molecular cannibalism: sacrificial materials as precursors for hollow and multidomain single crystals. *Nat. Commun.* **2021**, *12*, 957.
(35) Srisanga, S.; Flood, A. E.; Galbraith, S. C.; Rugmai, S.; Soontaranon, S.; Ulrich, J. Crystal growth rate dispersion versus size-dependent crystal growth: appropriate modeling for crystallization processes. *Cryst. Growth Des.* **2015**, *15*, 2330−2336.
(36) Shtukenberg, A. G.; García-Ruiz, J. M.; Kahr, B. Punin ripening and the classification of solution-mediated recrystallization mechanisms. *Cryst. Growth Des.* **2021**, *21*, 1267−1277.
(37) Baglai, I.; Leeman, M.; Wurst, K.; Kaptein, B.; Kellogg, R. M.; Noorduin, W. L. The Strecker reaction coupled to Viedma ripening: a simple route to highly hindered enantiomerically pure amino acids. *Chem. Commun.* **2018**, *54*, 10832−10834.
(38) van Dongen, S. W.; Maeda, J.; Kaptein, B.; Cardinael, P.; Flood, A. E.; Coquerel, G.; Noorduin, W. L. Mechanistic dissymmetry between crystal growth and dissolution drives ratcheted chiral amplification. *J. Am. Chem. Soc.* **2025**, *147*, 38508−38515.
(39) Guillaneux, D.; Zhao, S. H.; Samuel, O.; Rainford, D.; Kagan, H. B. Nonlinear effects in asymmetric catalysis. *J. Am. Chem. Soc.* **1994**, *116*, 9430−9439.
(40) Lewis, A.; Seckler, M. M.; Kramer, H. J. M.; van Rosmalen, G. M. *Industrial Crystallization: Fundamentals and Applications*; Cambridge University Press, 2015. DOI: 10.1017/CBO9781107280427.
(41) The calculations overestimate the effects observed experimentally, since they do not account for size and shape evolution. Although all crystals grow, the smaller crystals grow in corporate relatively much more mass per crystal compared to larger crystals. Consequently, the size disparity shrinks over time. Hence the integrated effects of size disparity over time are lower than purely expected based on its initial imbalance.
(42) Winn, D.; Doherty, M. F. Modeling crystal shapes of organic materials grown from solution. *AIChE J.* **2000**, *46*, 1348−1367.
(43) Lu, F.; Zhang, Y.; Zhang, L.; Su, D.; Zhuang, Z.; Liu, M.; Chen, J. G.; Gang, O. Continuous encodable reshaping of gold nanocrystals through facet modulation. *J. Am. Chem. Soc.* **2025**, *147*, 25871−25882.
(44) Sacchi, P.; Neoptolemou, P.; Davey, R. J.; Reutzel-Edens, S. M.; Cruz-Cabeza, A. J. Do metastable polymorphs always grow faster? Measuring and comparing growth kinetics of three polymorphs of tolfenamic acid. *Chem. Sci.* **2023**, *14*, 11775−11789.
(45) Ma, C. Y.; Wang, X. Z.; Roberts, K. J. Multi-dimensional population balance modeling of the growth of rod-like L-glutamic acid crystals using growth rates estimated from in-process imaging. *Adv. Powder Technol.* **2007**, *18*, 707−723.
(46) Suwannasang, K.; Flood, A. E.; Rougeot, C.; Coquerel, G. Use of programmed damped temperature cycles for the deracemization of a racemic suspension of a conglomerate forming system. *Org. Process Res. Dev.* **2017**, *21*, 623−630.
(47) Bodák, B.; Maggioni, G. M.; Mazzotti, M. Effect of initial conditions on solid-state deracemization via temperature cycles: a model-based study. *Cryst. Growth Des.* **2019**, *19*, 6552−6559.
(48) Gherase, D.; Conroy, D.; Matar, O. K.; Blackmond, D. G. Experimental and theoretical study of the emergence of single chirality in attrition-enhanced deracemization. *Cryst. Growth Des.* **2014**, *14*, 928−937.
(49) Noorduin, W. L.; Meekes, H.; van Enckevort, W.; J, P.; Kaptein, B.; Kellogg, R. M.; Vlieg, E. Enantioselective symmetry breaking directed by the order of process steps. *Angew. Chem., Int. Ed.* **2010**, *49*, 2539−2541.
(50) Belletti, G.; Schuurman, J.; Meekes, H.; Rutjes, F. P. J. T.; Vlieg, E. Combining Viedma ripening and temperature cycling deracemization. *Cryst. Growth Des.* **2022**, *22*, 1874−1881.

https://doi.org/10.1021/acs.jpclett.5c03059
J. Phys. Chem. Lett. XXXX, XXX, XXX−XXX

(51) Kondepudi, D. K.; Crook, K. E. Theory of conglomerate crystallization in the presence of chiral impurities. *Cryst. Growth Des.* **2005**, *5*, 2173−2179.
(52) Sangwal, K. Effect of impurities on the processes of crystal growth. *J. Cryst. Growth* **1993**, *128*, 1236−1244.
(53) Cameli, F.; ter Horst, J. H.; Steendam, R. R. E.; Xiouras, C.; Stefanidis, G. D. On the effect of secondary nucleation on deracemization through temperature cycles. *Chem.—Eur. J.* **2020**, *26*, 1344−1354.
(54) Beckmann, W. Seeding the desired polymorph: background, possibilities, limitations, and case studies. *Org. Process Res. Dev.* **2000**, *4*, 372−383.
(55) McDonald, M. A.; Salami, H.; Harris, P. R.; Lagerman, C. E.; Yang, X.; Bommarius, A. S.; Grover, M. A.; Rousseau, R. W. Reactive crystallization: a review. *React. Chem. Eng.* **2021**, *6*, 364−400.
(56) Viedma, C.; Ortiz, J. E. A new twist in eutectic composition: deracemization of a racemic compound amino acid by Viedma ripening and temperature fluctuation. *Isr. J. Chem.* **2021**, *61*, 758−763.
(57) Pinetre, C.; van Dongen, S. W.; Brandel, C.; Léonard, A. S.; Charpentier, M. D.; Dupray, V.; Oosterling, K.; Kaptein, B.; Leeman, M.; Kellogg, R. M.; ter Horst, J. H.; Noorduin, W. L. Enantiopurity by directed evolution of crystal stabilities and nonequilibrium crystallization. *J. Am. Chem. Soc.* **2025**, *147*, 8864−8870.
(58) Katsuno, H.; Uwaha, M. How do most stable racemic crystals transform into metastable chiral crystals by grinding? *Cryst. Growth Des.* **2025**, *25*, 3735−3741.
(59) Ślęczkowski, M. L.; Mabesoone, M. F. J.; Ślęczkowski, P.; Palmans, A. R. A.; Meijer, E. W. Competition between chiral solvents and chiral monomers in the helical bias of supramolecular polymers. *Nat. Chem.* **2021**, *13*, 200−207.
(60) Yang, S.; Geiger, Y.; Geerts, M.; Eleveld, M. J.; Kiani, A.; Otto, S. Enantioselective self-replicators. *J. Am. Chem. Soc.* **2023**, *145*, 16889−16898.
(61) Ernst, K. H. Supramolecular surface chirality. *Top. Curr. Chem.* **2006**, *265*, 209−252.
(62) Palmans, A. R. A.; Meijer, E. W. Amplification of chirality in dynamic supramolecular aggregates. *Angew. Chem., Int. Ed.* **2007**, *46*, 8948−8968.
(63) Feringa, B. L.; van Delden, R. A. Absolute asymmetric synthesis: the origin, control, and amplification of chirality. *Angew. Chem., Int. Ed.* **1999**, *38*, 3418−3438.

https://doi.org/10.1021/acs.jpclett.5c03059
J. Phys. Chem. Lett. XXXX, XXX, XXX−XXX